

ALMA Memo 423

The Vane Calibration System revisited

S.Guilloteau (IRAM / ESO)

May 27, 2002

Abstract

I re-investigate the semi-transparent vane calibration scheme proposed for ALMA, taking into account expected saturation behavior of the receivers. This memo improves on [Guilloteau & Moreno, memo 371] by using more accurate derivations and better estimates of the receiver saturation temperatures. It is shown that to reach a given precision in calibration, the saturation on the vane must be less than this precision. Suitable values for the vane transparencies are given. The vane transmission can be calibrated in a few minutes (at mm wavelengths) to 1 hour (above 275 GHz) by measurement of an astronomical source (nearby quasar). A derivation of the saturation temperature from a measurement on the vane and on an ambient load is presented. The case of partial saturation on the vane is explored. Using the derived saturation temperature in this case requires a more accurate measurement of the vane transmission, but is the only way to reach the specified accuracy. Given the simplicity of the vane system (passive, slow device, in the receiver cabin), compared with the complexity, speed and location of the dual-load system, I recommend that ALMA develops and adopts such a scheme for the receiver calibration.

1 Basic System Noise

The typical system temperature is derived from the agreed ALMA specifications, in the same way as in [Moreno & Guilloteau, memo 372]. I assume the standard ALMA numbers:

$$T_{\text{rec}}(\nu) = 6h\nu/k + 4 \text{ K} \quad (\nu < 400\text{GHz}) \quad \text{and} \quad T_{\text{rec}}(\nu) = 10h\nu/k + 4 \text{ K} \quad (\nu > 400\text{GHz})$$

for single sideband receivers (rejection better than 10 dB).

$$T_{\text{rec}}(\nu) = 3h\nu/k \text{ K} \quad (\nu < 400\text{GHz}) \quad \text{and} \quad T_{\text{rec}}(\nu) = 5h\nu/k \text{ K} \quad (\nu > 400\text{GHz})$$

for double sideband receivers. This ignores (for simplicity) more subtle dependence with frequency (specially for Band 7). I also assume the forward efficiency is falling down from 0.95 at low frequencies to 0.90 at 900 GHz (as ν^2).

The atmospheric conditions are taken from the weather statistics percentiles, with temperature adjusted to account (to first order) for the imperfect correlation between temperature and opacity. We assume dynamic scheduling will match the observed frequency to the appropriate observing conditions, more precisely that observations above 370 GHz will be done only in the 25 % best observing time, observations between 270 and 370 GHz only in the 50 % best observing time, and “low” frequency observations in the remaining available good weather (see Table 1). Figure 1 gives the corresponding expected system temperature **in the receiver calibration plane, for continuum observations, i.e.**

$$T_{\text{ant}} = T_{\text{rec}} + J_{\text{sky}} \tag{1}$$

(see Eq.4 for the complete expression of J_{sky}). T_{ant} is the relevant quantity to compare with load temperatures, rather than the more usual Single Sideband system temperature outside the atmosphere, which is only relevant for the astronomical observations of spectral lines.

Percentile	$\tau(225 \text{ GHz})$	Water vapor		Temperature	Observing Frequency
		Max.	Typical		
75 %	0.117	< 2.3 mm	2.3 mm	+3°C	< 250 GHz
50 %	0.061	< 1.2 mm	1.0 mm	0°C	< 370 GHz
25 %	0.037	< 0.7 mm	0.5 mm	-5°C	700 GHz

Table 1: Adopted percentiles for the computation of the system temperatures. Note that this differs from individual percentiles by trying (grossly) to account for correlations between opacity and temperature.

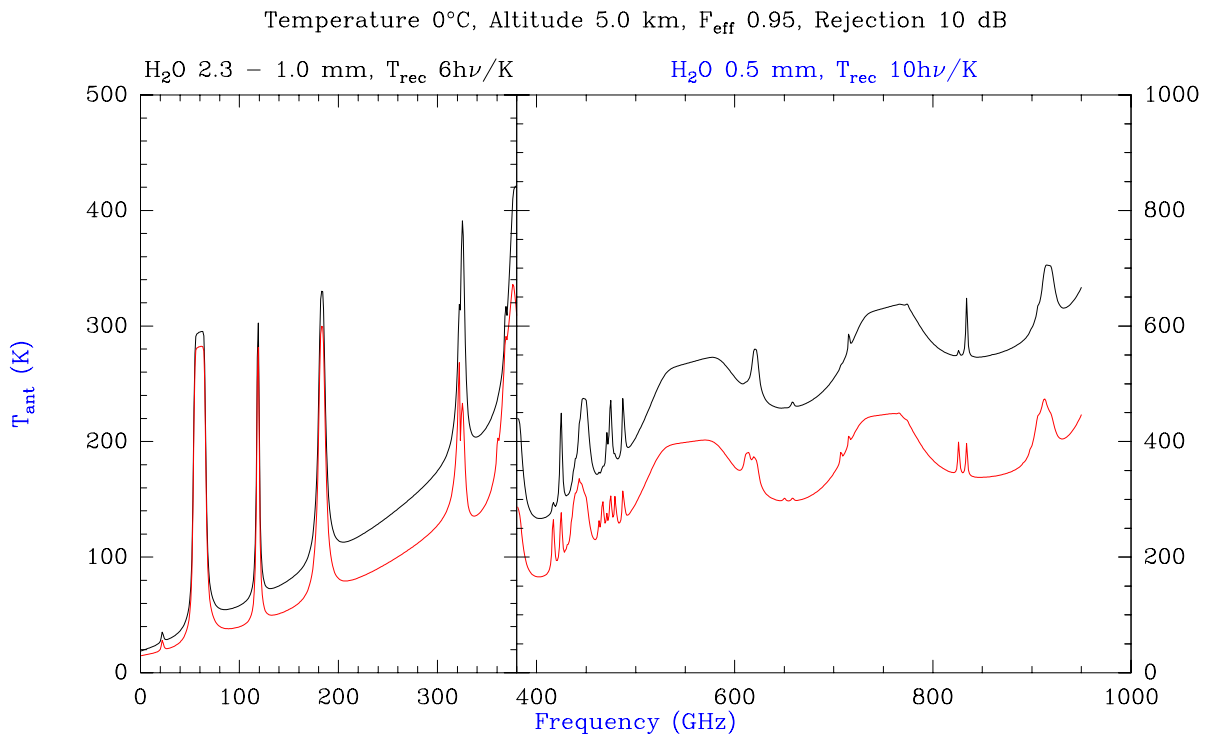


Figure 1: Expected typical antenna plane system temperatures with ALMA, for continuum observations. The black curves correspond to Single Side Band tuned receivers (image rejection 10 dB), while the red curves correspond to Double Side Band tuned receivers. Since SSB receivers have twice less bandwidth, there corresponding system temperature is $\simeq \sqrt{2}$ worse than that of DSB receivers. Created by `default_tant.astro`

2 Basic Equations

2.1 Standard Chopper / Vane Calibration

The calibration can be derived from the output powers measured by the receiver on the sky P_{sky} and when looking at a load P_{load} , compared to the correlated signal measured by the

correlator, C_{source} :

$$\begin{aligned} P_{\text{sky}} &= K(P_{\text{sky}})(T_{\text{rec}} + J_{\text{sky}}) \\ P_{\text{load}} &= K(P_{\text{load}})(T_{\text{rec}} + fJ_{\text{load}} + (1-f)J_{\text{sky}}) \\ C_{\text{source}} &= K(P_{\text{sky}})g_s\eta e^{-\tau}T_A \end{aligned} \quad (2)$$

The coefficient $K(P)$ incorporates possible non linearity of the detector (receiver + amplifiers + backend). f is the fraction of the beam filled by the load, and η the forward efficiency. g_s and g_i are the normalized signal and image gain of the receivers $g_s + g_i = 1$. Note that, in terms of image to signal gain ratio, g ,

$$g_s = 1/(1+g) \quad \text{and} \quad g_i = g/(1+g) \quad (3)$$

The sky emissivity J_{sky} is given by

$$\begin{aligned} J_{\text{sky}} &= g_s(\eta J_{\text{m}}^s(1 - e^{-\tau_s}) + \eta J_{\text{bg}}^s e^{-\tau_s} + (1-\eta)J_{\text{spill}}^s) \\ &\quad + g_i(\eta J_{\text{m}}^i(1 - e^{-\tau_i}) + \eta J_{\text{bg}}^i e^{-\tau_i} + (1-\eta)J_{\text{spill}}^i) \end{aligned} \quad (4)$$

where τ_j is the sky opacity (at the current elevation) and

$$J_{\text{x}}^j = \frac{h\nu_j}{k} \frac{1}{e^{h\nu_j/kT_{\text{x}}} - 1} \quad (5)$$

is the Rayleigh-Jeans equivalent temperature of a black body at T_{x} at frequency ν_j . j takes values s or i for signal or image bands respectively. J_{m} is the effective atmospheric temperature (source function), J_{bg} the cosmic background, and J_{spill} the spillover. Similarly, the effective load temperature J_{load} is

$$J_{\text{load}} = g_s J_{\text{load}}^s + g_i J_{\text{load}}^i \quad (6)$$

A major limitation of the calibration accuracy is the possible saturation of the receiver when looking at a warm load (or at the sky...). From [Plambeck memo 321], the saturation curve can be expressed as

$$K(P) = \frac{K_0}{1 + P_{\text{ant}}/P_{\text{sat}}} \quad (7)$$

where, for SIS receivers, the saturation power P_{sat} is given by

$$P_{\text{sat}} = C_{\text{sat}} \frac{N^2 \nu^2}{G_0 R_L} \quad (8)$$

$$C_{\text{sat}} = \frac{1}{8} \left(\frac{h}{e} \right)^2 = 2.12 \cdot 10^{-30} \quad (9)$$

N is the number of junctions, ν is the frequency (Hz), G_0 is the receiver conversion gain, R_L is the receiver impedance (Ω) [Tucker & Feldman 1985] [Kerr memo 401]. In comparison, the input power from a load at temperature T is given by

$$P_{\text{in}} = kT\Delta\nu \quad (10)$$

where $\Delta\nu$ is the **input bandwidth** of the receiver.

In terms of noise equivalent temperatures, we can thus define $T_{\text{sat}} = P_{\text{sat}}/(k\Delta\nu)$, where $\Delta\nu$ is the **input bandwidth** of the receiver. We can now derive the **saturation temperature** of the receiver as

$$T_{\text{sat}} = \frac{P_{\text{sat}}}{k\Delta\nu} = \frac{C_{\text{sat}}}{k\Delta\nu} \frac{N^2 \nu^2}{G_0 R_L} \quad (11)$$

The receiver saturation (Eq.7) can thus be re-expressed as

$$K(T) = \frac{K_0}{1 + (J_{\text{ant}}/T_{\text{sat}})} \quad (12)$$

Note that in Eq.12, J_{ant} is not T_{ant} , but the **input equivalent noise temperature**, and should in principle not incorporate the self-generated noise from the receiver. Thus, $T_{\text{ant}} = T_{\text{rec}} + J_{\text{ant}}$, provided T_{rec} is measured at the entrance of the mixer... T_{ant} should be used for noise determination, while J_{ant} should be used for saturation effects. In practice, T_{rec} is normally measured at the entrance of the dewar, so that it does include some input noise to the mixer. A proper treatment of the saturation of the mixer would require to incorporate such noise contributions (from the losses in the internal optics of the receiver) into J_{ant} . Note also that Eq.12 does not handle the case of compression into the IF chain.

The saturation temperature of the receiver depends on 4 parameters:

- **Input Bandwidth** Evaluating the input bandwidth $\Delta\nu$ of the receiver is not so obvious. This bandwidth is at least equal to the output bandwidth, but may not be much larger because of the impedance mismatch at the junction way off the tuning frequency. I assume the input bandwidth is twice the highest IF frequency delivered by the receiver: $\Delta\nu = 24$ GHz or $\Delta\nu = 16$ GHz depending on the option of the IF (4-12 GHz, or 4-8 GHz).
- **Impedance** The typical impedance R_L is 50 Ω .
- **Conversion Gain** For simplicity, I also assume the conversion gain $G_0 = 1$; this is probably an upper limit for most practical mixers, although SIS mixers can in theory provide conversion gain.
- **Number of junctions** In the current proposed designs for ALMA, $N = 4$ for bands 3 and 6, and $N = 1$ for bands 7 and 9.

Inserting all assumed numbers give

$$T_{\text{sat}} \simeq 20000 \left(\frac{\nu}{100 \text{ GHz}} \right)^2 \text{ K} \quad \text{for band 3 and 6} \quad (13)$$

$$T_{\text{sat}} \simeq 1300 \left(\frac{\nu}{100 \text{ GHz}} \right)^2 \text{ K} \quad \text{for band 7 and 9} \quad (14)$$

Saturation is maximal at the lowest frequencies in each band. For band 3 at 84 GHz, $T_{\text{sat}} = 14000$ K, leading to a saturation of 2.1 % on an ambient load. For band 7 at 275 GHz, $T_{\text{sat}} = 9700$ K and the saturation would be 3.1 % on an ambient load.

Two strategies have been proposed to minimize this non linearity problem: the dual-load calibration in the subreflector [Bock et al. memo 225], or the semi-transparent vane [Plambeck memo 321]. A similar system was actually used on the IRAM Plateau de Bure antennas: the warm load could be inserted so as to cover partially the beam of the receiver. This particular system was not extremely accurate because of the asymmetric blockage of the aperture. An homogeneous semi-transparent vane covering the whole beam is much preferable. An initial comparison between the two devices was presented in [Guilloteau & Moreno, memo 371]. A more accurate study of the requirements for a dual load calibration system is presented in [Guilloteau, memo 422]. This memo deals with the requirements on the semi-transparent vane.

3 Semi Transparent Vane

3.1 Vane Absorption Value

For the semi-transparent vane calibration method, the measurement equations are

$$\begin{aligned} P_{\text{sky}} &= K(P_{\text{sky}})(T_{\text{rec}} + J_{\text{sky}}) \\ P_{\text{vane}} &= K(P_{\text{vane}})(T_{\text{rec}} + fJ_{\text{load}} + (1-f)J_{\text{sky}}) \\ C_{\text{source}} &= K(P_{\text{sky}})\eta e^{-\tau}T_A \end{aligned} \quad (15)$$

If $K(P)$ is assumed constant, this is a one-load calibration method, for which the source antenna temperature is given by

$$T_A = fT_{\text{cal}} \frac{C_{\text{source}}}{P_{\text{vane}} - P_{\text{sky}}} \quad (16)$$

where T_{cal} is the calibration temperature [Ulich & Haas, 1976]

$$\begin{aligned} T_{\text{cal}} &= J_{\text{spill}}^s - J_{\text{bg}}^s + g(J_{\text{spill}}^i - J_{\text{bg}}^i) \\ &+ (e^{\tau_s} - 1)(J_{\text{spill}}^s - J_{\text{m}}^s + g(J_{\text{spill}}^i - J_{\text{m}}^i)) \\ &+ g(e^{\tau_s - \tau_i} - 1)(J_{\text{m}}^i - J_{\text{bg}}^i) \\ &+ \frac{e^{\tau_s}}{\eta}(J_{\text{load}}^s - J_{\text{spill}}^s + g(J_{\text{load}}^i - J_{\text{spill}}^i)) \end{aligned} \quad (17)$$

The expression of T_{cal} , although complex, has two useful limiting cases: the homogeneous temperature case $J_{\text{load}} \simeq J_{\text{m}} \simeq J_{\text{spill}}$ for which

$$T_{\text{cal}} \simeq (1 + ge^{\tau_s - \tau_i})(J_{\text{m}} - J_{\text{bg}}) \quad (18)$$

and the low opacity case $\tau \ll 1$, for which

$$T_{\text{cal}} \simeq \frac{1+g}{\eta}(J_{\text{load}} - (1-\eta)J_{\text{spill}}) \quad (19)$$

Note that in Eq.15, the receiver temperature T_{rec} is a self-generated noise, and in principle not subject to the same saturation as the input noise. I shall ignore this slight complication. . . Eq.16 is only valid if $K(J_{\text{sky}}) = K(J_{\text{vane}})$. If not Eq.16 becomes

$$T_A = fT_{\text{cal}} \frac{C_{\text{source}}}{P_{\text{vane}} \frac{K(J_{\text{sky}})}{K(J_{\text{vane}})} - P_{\text{sky}}} \quad (20)$$

which after some re-arrangement detailed in Appendix A becomes

$$T_A = fT_{\text{cal}} \frac{C_{\text{source}}}{P_{\text{vane}} - P_{\text{sky}} + f \frac{P_{\text{vane}}(J_{\text{load}} - J_{\text{sky}})}{T_{\text{sat}} + J_{\text{sky}}}} \quad (21)$$

Hence, ignoring the correction for saturation at some level y requires $\delta T_A/T_A < y$, which is demonstrated in Appendix B to be equivalent to

$$\frac{J_{\text{vane}}}{T_{\text{sat}}} \leq y \quad (22)$$

This shows that saturation on the load must be less than the required precision y to offer a solution to the problem. In particular, because of the shape of the saturation function, it is

not sufficient to have compression factors $K(J_x)$ equals to the required precision on sky and on load, since we use the difference signal for the calibration. Using the complete expression of J_{vane} gives

$$f(J_{\text{load}} - J_{\text{sky}}) + J_{\text{sky}} \leq yT_{\text{sat}} \quad (23)$$

and finally

$$f \leq \frac{yT_{\text{sat}} - J_{\text{sky}}}{J_{\text{load}} - J_{\text{sky}}} \quad (24)$$

In practice, only loads at the ambient temperature can have an accurately defined effective temperature J_{load} , for which a 0.5°C temperature error result in 0.2 % uncertainty. Loads at other temperatures must be insulated to avoid temperature gradients at the load surface, but such an insulation requires an infrared shield. The uncertainty in the reflection coefficient of this insulation layer at mm or submm wavelengths could dominate the calibration accuracy. Moreover, a fixed temperature error result in a larger relative error on J_{load} at lower load temperatures.

It is clear from Eq.24 that the biggest problem, i.e. the lowest values of f , in general occur at the longest wavelengths for each receiver band, because the lower values of T_{sat} (see Eq.7-8) and J_{sky} concur to minimize the allowed value of f . More serious problems can also happen when J_{sky} becomes too large, i.e. near absorption lines of the atmosphere; however, saturation will not be the more serious issue in such cases.

Limiting the saturation to $y = 0.8\%$, the values of f as function of frequency and saturation temperature T_{sat} are displayed in Fig.2, for values around the expected saturation temperatures of the ALMA receivers. The abrupt change at 275 GHz is due to the transition from Band 6 (with 4 junctions) to Band 7 (with only 1 junction).

We can neglect the noise on the measurement, since the precision in $P_{\text{load}} - P_{\text{sky}}$ obtained in a time t is (for $K(J_{\text{vane}}) = K(J_{\text{sky}})$)

$$z \approx \frac{2 T_{\text{ant}}}{\sqrt{\Delta\nu t}} \frac{1}{f(J_{\text{load}} - J_{\text{sky}})} \quad (25)$$

$$t \approx \frac{4}{\Delta\nu} \left(\frac{T_{\text{ant}}}{z f(J_{\text{load}} - J_{\text{sky}})} \right)^2 \quad (26)$$

which is much less than 0.1 s, in all circumstances. This integration time is given in Fig.3.1 for 100 MHz bandwidth.

3.2 Vane Absorption Calibration

A big advantage of the semi-transparent vane calibration system resides in the possibility to accurately calibrate the absorption coefficient f by observing a source with or without the vane in front of the receiver. Since we have allowed $y = 0.8\%$ for the saturation, f must be measured with 0.5 % accuracy to remain consistent with our goal of 1% total error. The integration time required to do so is an interesting parameter, because if it is short enough, it is possible to have the vane moved by a (relatively) slow and simple system. If not, the vane must be mounted on some chopping system to provide periods of order of a few seconds. This is to guarantee stable statistical properties of the atmospheric conditions between the on-vane and off-vane observations, both in transmission and phase noise.

To estimate this integration time, we use the antenna-based noise equivalent flux S_0 as derived by [Moreno & Guilloteau, memo 372], and consider that we can move to a source of

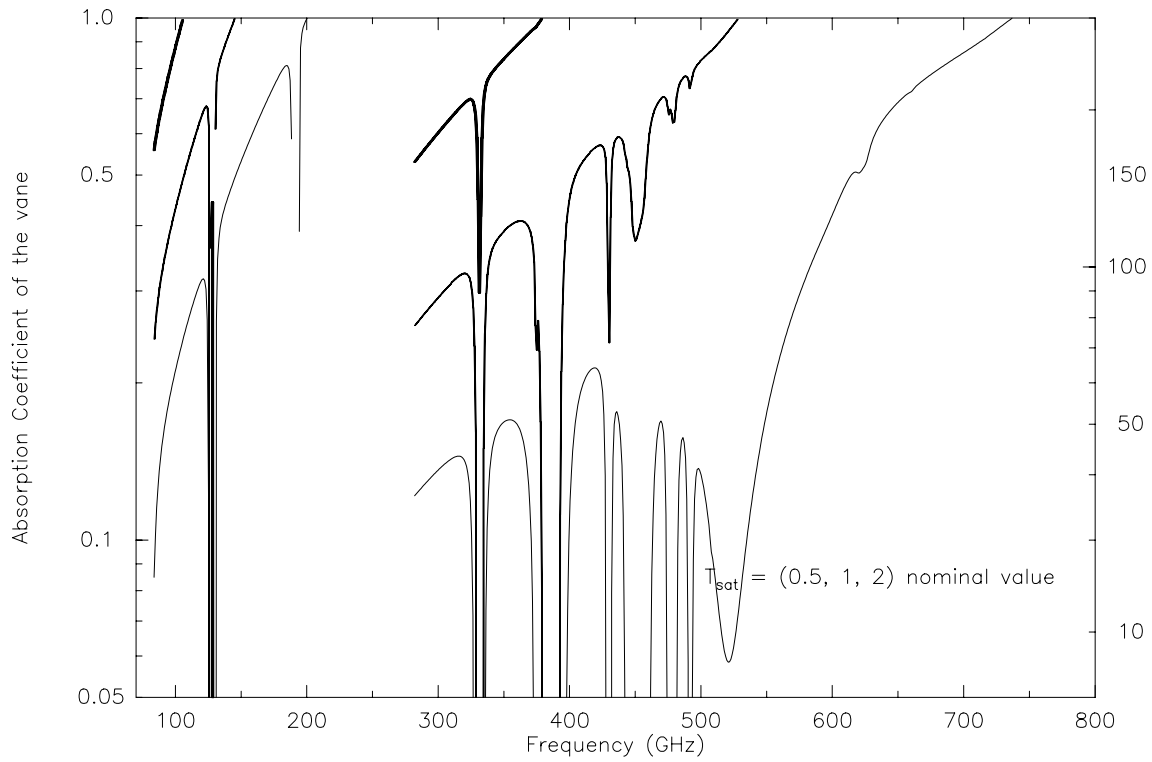


Figure 2: Maximum vane absorption coefficient f as a function for frequency. The three curves, from thin to thick, are for $T_{\text{sat}} = 0.5, 1, 2$ times the nominal value for each band. The right axis indicate the effective load temperature (K).

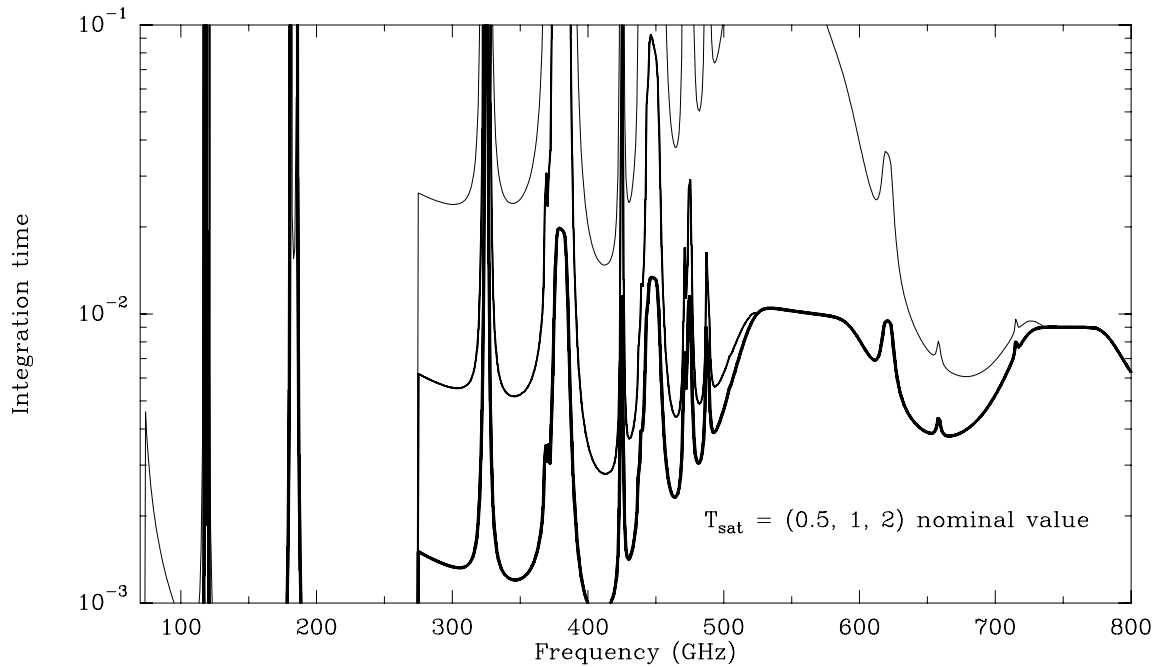


Figure 3: Integration time to measure T_{cal} with 0.5 % precision due to radiometric noise

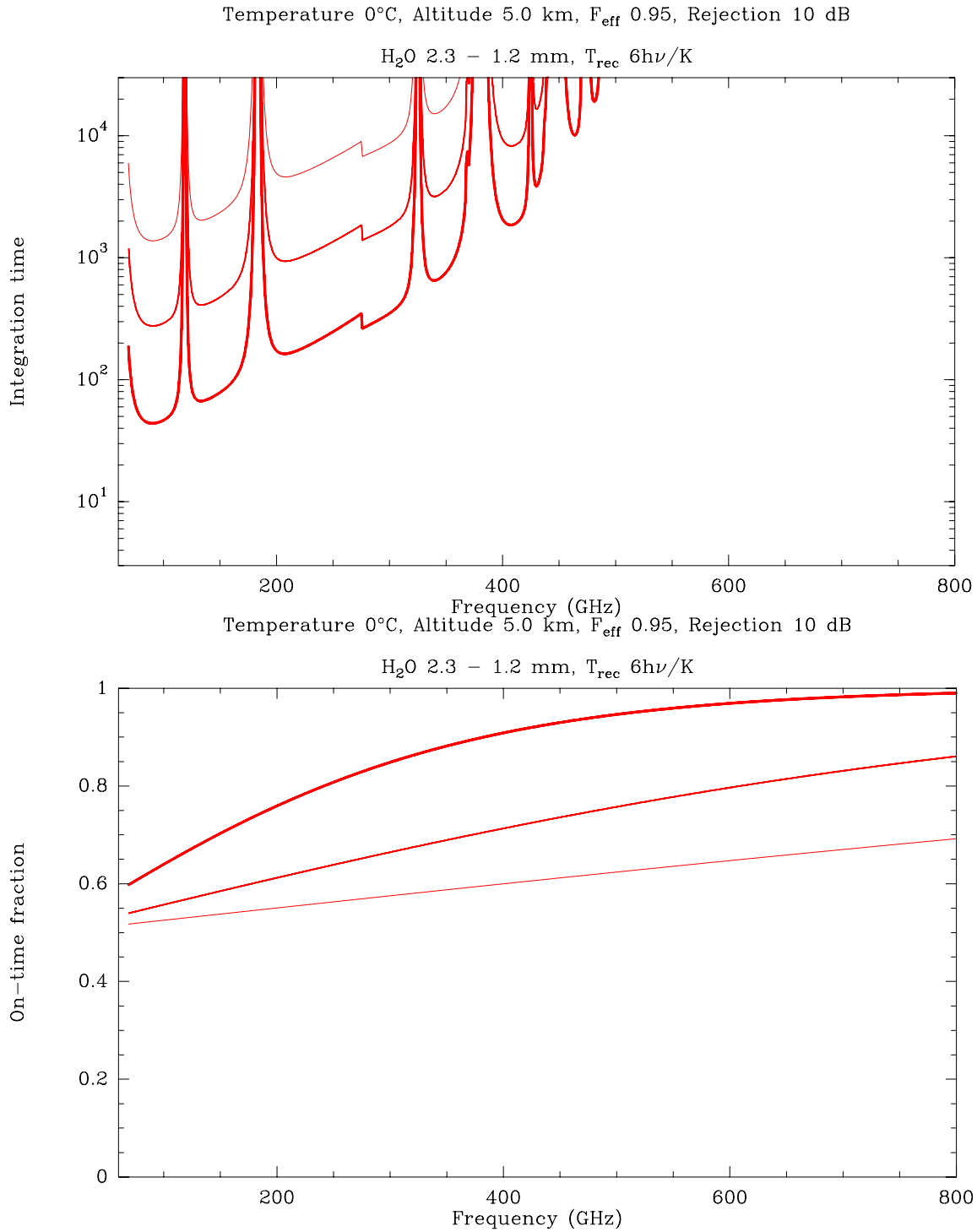


Figure 4: Top: Integration time to measure the absorption coefficient f with 0.5 % accuracy on a typical quasar with 8 GHz bandwidth (or equivalently on a bandpass calibrator with 500 MHz bandwidth). The three curves, from thin to thick, are for T_{sat} ranging from 0.5, 1, 2 times the nominal value is used. The vane is optimized for 280 GHz observations. Bottom: Fraction of time spent vane on during the vane calibration.

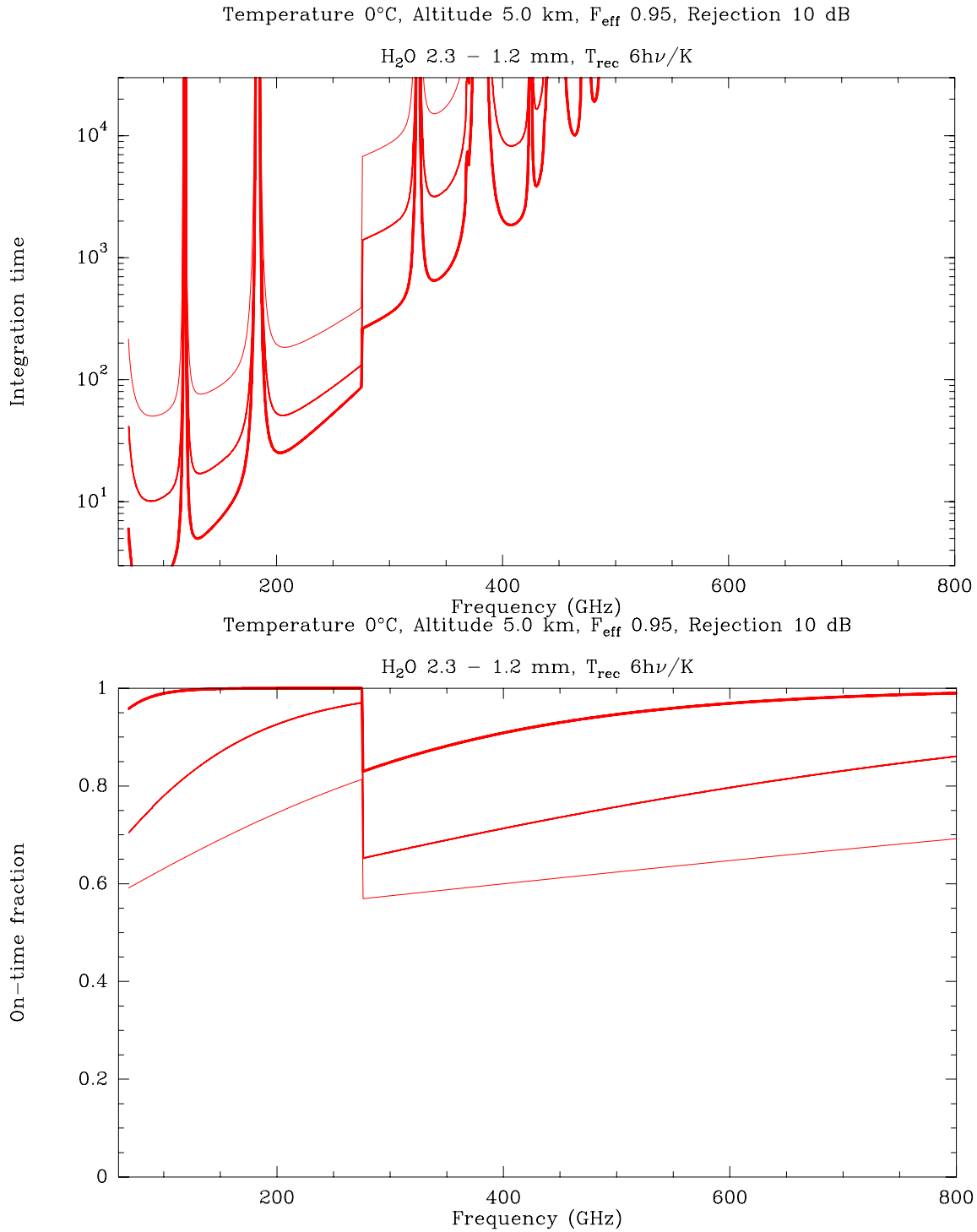


Figure 5: Top: Integration time to measure the absorption coefficient f with 0.5 % accuracy on a typical quasar with 8 GHz bandwidth (or equivalently on a bandpass calibrator with 500 MHz bandwidth). The three curves, from thin to thick, are for T_{sat} ranging from 0.5, 1, 2 times the nominal value is used. Two vanes, one optimized for 86 GHz observations and one for 280 GHz observations are considered. Bottom: Fraction of time spent vane on during the vane calibration.

flux S to perform this measurement. Let $x = 1 - f$ be the transmission coefficient of the vane. The vane-on signal is xS , while the vane-off signal is S . To equalize the error terms on the ratio of the two measurements, S and xS , we need to spend $t_{\text{on}} = t/(1 + x^2)$ with the vane on, and only $t_{\text{off}} = tx^2/(1 + x^2)$ with the vane off for a total time t , and the resulting error is

$$\frac{\delta x}{x} = \frac{2\sqrt{1 + x^2}S_0}{Sx\sqrt{t\Delta\nu}} \quad (27)$$

which, when converted to f , results in

$$\frac{\delta f}{f} = \frac{2\sqrt{1 + (1 - f)^2}S_0}{Sf\sqrt{t\Delta\nu}} \quad (28)$$

or z being the required precision in $\delta f/f$

$$t = \frac{1}{\Delta\nu} \frac{4(1 + (1 - f)^2)S_0^2}{z^2 f^2 S^2} \quad (29)$$

Figure 4-5 gives the resulting integration time as function of frequency, and the fraction of time spent vane on, for $\Delta\nu = 8$ GHz. The calibration source is a quasar of 1.5 Jy, and spectral index -0.7 , which can be found within 5 degrees of any source. Fig.4 considers the case where only one vane is build, with an absorption coefficient matched to the required value at 280 GHz. Fig.5 considers the case with 2 vanes, one matched to 280 GHz, the other one matched to 86 GHz. In both cases, a “normal” lossy material with an absorption coefficient proportional to the frequency has been assumed, i.e. that the vane absorption coefficient varies as $f(\nu) = (1 - \exp(-f_0\nu))$.

If only one vane covering all frequencies is build, it must be designed to handle the worst case, i.e. saturation at 280 GHz. Fig.2 indicates its absorption coefficient should be at most 0.2–0.3 at this frequency. With an absorption proportional to the frequency, the absorption becomes very small at 90 GHz. Fig.4 indicates that the time required to calibrate the vane transmission f to 0.5 % accuracy ranges from 1 minute at 90 GHz to 1 hour at 350 GHz, depending on frequencies and assumed saturation temperature, and becomes prohibitive at sub-mm wavelengths.

Using a stronger quasar (bandpass calibrator for example), these integration times can be reduced by a factor 16. However, using the full bandwidth of 8 GHz may not be adequate because of the frequency dependence of f , specially due to possible standing waves. Standing waves between the receiver and the vane will produce ripples with period of order several hundred MHz. Integration needs to be 16 times longer for $\Delta\nu = 500$ MHz than for 8 GHz, compensating the gain expected by going to a stronger calibrator.

These long times occur because the useful signal is $(1 - f)S$ instead of S as assumed by [Plambeck memo 321], while the required precision on that signal goes as $1/f$. If two vanes are build, one can cover Band 3 to 6, with an absorption coefficient of order 0.2 at 90 GHz. The time required for calibration becomes quite small, of order a few seconds up to Band 6 edge. No change occurs for Band 7 (see Fig.5) and beyond.

An additional problem which must be worked out is the possible different decorrelation factors on the vane-on and vane-off measurement, due to the different integration times. For long timescales, there is actually a component of the WVR correction which depends on the initial error, due to the limited accuracy of the prediction. Assuming a 10% accuracy for the correction, an estimate to this residual error is given by

$$\Delta P = 0.1\sigma_w (\min(B, vt)/300)^{0.6} \mu\text{m} \quad (30)$$

where t is the timescale, v the wind speed, and B the typical baseline length. Since $B < vt$ and $B \leq 1$ km except on the largest configuration (where the outer scale of the atmosphere would limit anyhow), we obtain $\Delta P \leq 25\mu\text{m}$, for which the decorrelation is 2.5 % at 300 GHz, but below 1 % at frequencies below 230 GHz. Since it is the variation of the decorrelation between the vane on and vane off positions which is important, these rather low values indicate that variable decorrelation should not be a severe issue.

Even taking into account the natural increase of the absorption coefficient with frequencies, Fig.4-5 indicate relatively long integration times to measure f , and definitely suggests two vanes offer a better solution. Since the absorption coefficient calibration time is significant near 300 GHz, we conclude that the commutation system should have a settling time of order 1 sec or less.

We note that with the assumed receiver parameters, saturation is a negligible problem in Band 6 with a 4 junction array. Having as less saturation as possible is always useful, since the time required to measure the vane absorption f is smaller for more opaque vanes (see Fig.4-5).

3.3 Saturation Temperature Determination

With one vane and an ambient load, some estimate of the saturation parameter is possible if J_{sky} is estimated independently, for example by an atmospheric model. Correction for saturation becomes possible in this case. From Eq.21, we derive for a measurement with a vane of absorption f

$$T_A(\text{vane}) = fT_{\text{cal}} \frac{C_{\text{source}}}{P_{\text{vane}} \left(1 + f \frac{J_{\text{load}} - J_{\text{sky}}}{T_{\text{sat}} + J_{\text{sky}}}\right) - P_{\text{sky}}} \quad (31)$$

while from a measurement on the ambient load (for which $f = 1$)

$$T_A(\text{load}) = T_{\text{cal}} \frac{C_{\text{source}}}{P_{\text{load}} \left(1 + \frac{J_{\text{load}} - J_{\text{sky}}}{T_{\text{sat}} + J_{\text{sky}}}\right) - P_{\text{sky}}} \quad (32)$$

Equating both quantities allows to estimate T_{sat} , which is given (for $f \neq 1$) by

$$T_{\text{sat}} = \frac{f(P_{\text{load}} - P_{\text{vane}})(J_{\text{load}} - J_{\text{sky}})}{P_{\text{vane}} - P_{\text{sky}} - f(P_{\text{load}} - P_{\text{sky}})} - J_{\text{sky}} \quad (33)$$

This is a useful check, since it allows to verify what is the actual level of saturation during the measurement, and correct for it. This is required when saturation on the vane exceeds the required precision (see Eq.24). In all cases, there is in principle a gain in precision by doing so. This improvement in precision is obtained by using the exact equation Eq.21, rather than the approximate formula Eq.16, and relaxes the need to avoid any saturation at all during the measurement.

This may also slightly relax the need to measure f with the required precision, by using the measurement on the ambient load (and the knowledge of T_{sat}) rather than the measurement on the vane (and the direct knowledge of f). Estimating the impact of inaccurate knowledge of f on T_{sat} and by inference on the calibration becomes cumbersome in analytical form. A complete derivation is given in Appendix C & D. The precision required on $1/(T_{\text{sat}} + J_{\text{sky}})$ to obtain a precision y on the calibration is (see Appendix C, Eq.64)

$$\frac{\delta \left(\frac{1}{T_{\text{sat}} + J_{\text{sky}}} \right)}{\left(\frac{1}{T_{\text{sat}} + J_{\text{sky}}} \right)} = y \frac{T_{\text{sat}} + J_{\text{sky}}}{J_{\text{load}}} \quad (34)$$

while the precision on $1/(T_{\text{sat}} + J_{\text{sky}})$ obtained from a measurement with the vane is related to the error on the vane absorption coefficient by (see Appendix D, Eq.77)

$$\frac{\delta \left(\frac{1}{T_{\text{sat}} + J_{\text{sky}}} \right)}{\left(\frac{1}{T_{\text{sat}} + J_{\text{sky}}} \right)} = \frac{\delta f}{f} \frac{T_{\text{sat}} + J_{\text{sky}}}{(1-f)(J_{\text{load}} - J_{\text{sky}})} \quad (35)$$

We thus derive that we need to know f with a relative precision

$$\frac{\delta f}{f} = y \frac{(1-f)(J_{\text{load}} - J_{\text{sky}})}{J_{\text{load}}} \quad (36)$$

i.e., in all cases, significantly better than y . This indirect method looks thus only a fall back when the saturation on the sky exceeds the precision required on the calibration. However, it should not be discarded so easily, because of effects related to the required spectral resolution in the measurement. Because of standing waves, f will have a frequency dependence on scales of a few 100 MHz, while T_{sat} is a single number characterizing the receiver (in its current tuning). It may be better for the point of view of bandpass calibration to use the indirect method with T_{sat} .

Note that the (relative) precision of the measurement of f is independent of f itself, since it is a relative calibration between the vane on and vane off. Finally, if J_{sky} is not known, 2 vanes would be required to determine also T_{rec} and J_{sky} . In a subsequent memo, it will be shown that accurate prediction of J_{sky} can be made in the mm regime.

4 Conclusions

The vane calibration system properties can be characterized by a few (simple) equations depending on the required precision level p . Simple calibration through a vane requires

1. No saturation

$$J_{\text{sky}} \leq y T_{\text{sat}} \quad (37)$$

2. i.e., a vane with absorption coefficient

$$f \leq \frac{y T_{\text{sat}} - J_{\text{sky}}}{J_{\text{load}} - J_{\text{sky}}} \quad (38)$$

3. and f measured with a relative precision better than z , where y and z must be chosen with $\sqrt{y^2 + z^2} \leq p$

If not, the saturation temperature T_{sat} can be derived by comparing the calibration with the vane and with an ambient load (see Eq.33), and correcting for saturation on the ambient load. This however requires to measure f with a relative precision better than

$$p \frac{(1-f)(J_{\text{load}} - J_{\text{sky}})}{J_{\text{load}}} \quad (39)$$

Table 2 summarizes the pro and cons of the vane calibration and of the dual-load in subreflector. The vane approach clearly offers a number of advantages, in terms of speed, calibration, and maintenance facility. One of the major issues is whether adequate material can be identified to produce such semi-transparent vanes. At the level of precision looked for, the exact nature

	Vane system	Dual-load
Location	In receiver cabin	<i>In subreflector</i>
Thermal control	At ambient, need measurement only	<i>Need heating system at 100° C in subreflector</i>
Speed	Slow device (1-2 sec)	<i>Fast switching (20-30 Hz)</i>
Reliability	Simple device	<i>Possible sealing problems at subreflector interface</i>
Maintenance	Easy access	<i>Awkward location</i>
Integration time	Short (< 1 sec)	<i>Up to 10 sec at submm frequencies</i>
Data Acquisition	Simple on 1 sec integration	<i>Requires demodulation scheme and synchronisation</i>
Basic Calibration	In a few minutes, on sky	<i>Not demonstrated</i>
Development	<i>to be done</i>	Prototype working
Standing Waves	minimal during observations	<i>Enhanced</i>
Spectral Resolution	Possible	<i>not possible</i>

Table 2: Pro and Con of the vane and dual-load calibration systems. **Pros** are in **boldface**, while *Cons* are in *italics*.

of the losses become important. The proposed scheme relies on the fact that the effective load temperature can be derived from the measurement of its transmission coefficient $(1 - f)$.

With better estimates of the saturation properties of the receivers, it becomes possible to make a specification for the vane transparencies. With the current knowledge, absorption coefficients of order 0.15 at the low frequency band edge are suitable for vanes in Band 3 and 7-8. Band 6 may work with only an ambient load. Such an ambient load is required for Band 9-10 any how, and allows improved correction for the saturation in case the semi-transparent vane is too absorbent. It also allows better calibration when saturation on the sky exceeds the precision for calibration.

All computations were made with a goal of 1 % precision on the calibration. This requires relatively long integration times above 275 GHz, and suggests that this goal will be difficult to achieve in Band 7. A less stringent goal of 3 % is more within reach.

Finally, one should mention that some astronomical sources will actually be strong enough to produce some receiver saturation. The Sun is one obvious case, but calibration accuracy is unlikely to be a real issue in this case. Jupiter and Venus are also too bright and will lead to some saturation. This is not a critical issue for imaging these objects, but prevent their use as primary calibrators, unless the correction for saturation is applied. Fortunately, among the possible primary flux calibrators such as Mars and Uranus, Mars hardly ever gets too bright at its most favorable opposition (less than a couple of weeks every 14 years) for the lowest saturation temperature, while Uranus is always weak enough.

Acknowledgements

This memo has benefitted from many useful discussions with Bernard Lazareff.

References

- [Mangum memo 318]
Mangum, J. 2000
Amplitude Calibration at Millimeter and Sub-millimeter Wavelengths *ALMA memo 318*
- [Plambeck memo 321]
Plambeck, R., 2000
Receiver Amplitude Calibration for ALMA *ALMA memo 321*
- [Bock et al. memo 225]
Bock, D., Welch, W.J., Fleming, M. & Thornton D., 1998
Radiometric Calibration at the Cassegrain Secondary Mirror *ALMA memo 225*
- [Tucker & Feldman 1985]
Tucker, J.R., Feldman, M.J. 1985
Quantum Detection at Millimeter Wavelengths
Review of Modern Physics, 57, 1055-1113
- [Ulich & Haas, 1976]
Ulich, R. & Haas, R.W., 1976
Amplitude Calibration of Millimeter Wavelengths Spectral Lines
ApJ Supp. 30, 247
- [Guilloteau & Moreno, memo 371]
Moreno, R., & Guilloteau, S. 2001,
Receiver Calibration Schemes for ALMA *ALMA memo 371*
- [Moreno & Guilloteau, memo 372]
Moreno, R., & Guilloteau, S. 2002,
ALMA Calibration: Requirements on the integration times, and suggested observing strategies. *ALMA memo 372*
- [Kerr memo 401]
Kerr, A.R., 2002
Saturation by Noise and CW Signals in SIS Mixers. *ALMA memo 401*
- [Guilloteau, memo 422]
Guilloteau S.,
The dual-load calibration system revisited. *ALMA memo 422*

A Appendix: Antenna temperature with saturation

If saturation cannot be neglected, the measurement equation becomes

$$T_A = fT_{\text{cal}} \frac{C_{\text{source}}}{P_{\text{vane}} \frac{K(P_{\text{sky}})}{K(P_{\text{vane}})} - P_{\text{sky}}} \quad (40)$$

whose denominator is

$$Z = P_{\text{vane}} \frac{K(P_{\text{sky}})}{K(P_{\text{vane}})} - P_{\text{sky}} \quad (41)$$

$$\frac{K(P_{\text{sky}})}{K(P_{\text{vane}})} = \frac{K(J_{\text{sky}})}{K(J_{\text{vane}})} = \frac{1 + J_{\text{vane}}/T_{\text{sat}}}{1 + J_{\text{sky}}/T_{\text{sat}}} = \frac{J_{\text{vane}} + T_{\text{sat}}}{J_{\text{sky}} + T_{\text{sat}}} \quad (42)$$

$$Z = P_{\text{vane}} \frac{J_{\text{vane}} + T_{\text{sat}}}{J_{\text{sky}} + T_{\text{sat}}} - P_{\text{sky}} \quad (43)$$

$$Z = \frac{P_{\text{vane}}(J_{\text{vane}} + T_{\text{sat}}) - P_{\text{sky}}(J_{\text{sky}} + T_{\text{sat}})}{J_{\text{sky}} + T_{\text{sat}}} \quad (44)$$

Developing $J_{\text{vane}} = fJ_{\text{load}} + (1 - f)J_{\text{sky}}$ gives

$$Z = \frac{P_{\text{vane}}((fJ_{\text{load}} + (1 - f)J_{\text{sky}}) + T_{\text{sat}}) - P_{\text{sky}}(J_{\text{sky}} + T_{\text{sat}})}{J_{\text{sky}} + T_{\text{sat}}} \quad (45)$$

$$Z = \frac{P_{\text{vane}}(J_{\text{sky}} + T_{\text{sat}}) + fP_{\text{vane}}(J_{\text{load}} - J_{\text{sky}}) - P_{\text{sky}}(J_{\text{sky}} + T_{\text{sat}})}{J_{\text{sky}} + T_{\text{sat}}} \quad (46)$$

$$Z = \frac{(P_{\text{vane}} - P_{\text{sky}})(J_{\text{sky}} + T_{\text{sat}}) + fP_{\text{vane}}(J_{\text{load}} - J_{\text{sky}})}{J_{\text{sky}} + T_{\text{sat}}} \quad (47)$$

$$Z = P_{\text{vane}} - P_{\text{sky}} + f \frac{P_{\text{vane}}(J_{\text{load}} - J_{\text{sky}})}{J_{\text{sky}} + T_{\text{sat}}} \quad (48)$$

hence

$$T_A = fT_{\text{cal}} \frac{C_{\text{source}}}{P_{\text{vane}} - P_{\text{sky}} + f \frac{P_{\text{vane}}(J_{\text{load}} - J_{\text{sky}})}{T_{\text{sat}} + J_{\text{sky}}}} \quad (49)$$

B Appendix: Maximum allowed saturation

To limit the effect of saturation to a precision y on the calibration accuracy thus requires the (unknown) correction term of Eq.49 to be smaller than y times the normal term:

$$f \frac{P_{\text{vane}}(J_{\text{load}} - J_{\text{sky}})}{T_{\text{sat}} + J_{\text{sky}}} \leq y(P_{\text{vane}} - P_{\text{sky}}) \quad (50)$$

$$f \frac{P_{\text{vane}}}{P_{\text{vane}} - P_{\text{sky}}} \leq y \frac{T_{\text{sat}} + J_{\text{sky}}}{J_{\text{load}} - J_{\text{sky}}} \quad (51)$$

which with $P_x = K(J_x)J_x$ becomes

$$f \frac{J_{\text{vane}}K(J_{\text{vane}})}{J_{\text{vane}}K(J_{\text{vane}}) - J_{\text{sky}}K(J_{\text{sky}})} \leq y \frac{T_{\text{sat}} + J_{\text{sky}}}{J_{\text{load}} - J_{\text{sky}}} \quad (52)$$

$$f \frac{J_{\text{vane}}}{J_{\text{vane}} - J_{\text{sky}} \frac{K(J_{\text{sky}})}{K(J_{\text{vane}})}} \leq y \frac{T_{\text{sat}} + J_{\text{sky}}}{J_{\text{load}} - J_{\text{sky}}} \quad (53)$$

which, reporting the expression of $K(J_{\text{sky}})/K(J_{\text{vane}})$ given in Eq.42 into Eq.53 leads to

$$f \frac{J_{\text{vane}}(T_{\text{sat}} + J_{\text{sky}})}{J_{\text{vane}}(T_{\text{sat}} + J_{\text{sky}}) - J_{\text{sky}}(T_{\text{sat}} + J_{\text{vane}})} \leq y \frac{T_{\text{sat}} + J_{\text{sky}}}{J_{\text{load}} - J_{\text{sky}}} \quad (54)$$

The denominator of the left hand side of this inequality is

$$Z = T_{\text{sat}}(J_{\text{vane}} - J_{\text{sky}}) = T_{\text{sat}}f(J_{\text{load}} - J_{\text{sky}}) \quad (55)$$

so that Eq.54 simplifies to

$$\frac{J_{\text{vane}}}{T_{\text{sat}}} \leq y \quad (56)$$

C Appendix: Direct saturation correction on ambient load

$$T_A(\text{load}) = T_{\text{cal}} \frac{C_{\text{source}}}{P_{\text{load}} \left(1 + \frac{J_{\text{load}} - J_{\text{sky}}}{T_{\text{sat}} + J_{\text{sky}}}\right) - P_{\text{sky}}} \quad (57)$$

T_0 being the true saturation temperature and T the derived one, the ratio of true versus predicted antenna temperature is given by

$$R = \frac{P_{\text{load}} \left(1 + \frac{J_{\text{load}} - J_{\text{sky}}}{T + J_{\text{sky}}}\right) - P_{\text{sky}}}{P_{\text{load}} \left(1 + \frac{J_{\text{load}} - J_{\text{sky}}}{T_0 + J_{\text{sky}}}\right) - P_{\text{sky}}} \quad (58)$$

$$R = 1 + \frac{P_{\text{load}} \left(1 + \frac{J_{\text{load}} - J_{\text{sky}}}{T + J_{\text{sky}}}\right) - P_{\text{sky}} - P_{\text{load}} \left(1 + \frac{J_{\text{load}} - J_{\text{sky}}}{T_0 + J_{\text{sky}}}\right) + P_{\text{sky}}}{P_{\text{load}} \left(1 + \frac{J_{\text{load}} - J_{\text{sky}}}{T_0 + J_{\text{sky}}}\right) - P_{\text{sky}}} \quad (59)$$

which simplifies to

$$R = 1 + \left(\frac{P_{\text{load}}(J_{\text{load}} - J_{\text{sky}})}{P_{\text{load}} \left(1 + \frac{J_{\text{load}} - J_{\text{sky}}}{T_0 + J_{\text{sky}}}\right) - P_{\text{sky}}} \right) \left(\frac{1}{T + J_{\text{sky}}} - \frac{1}{T_0 + J_{\text{sky}}} \right) \quad (60)$$

but, because of the shape of the saturation function,

$$\frac{P_{\text{load}}(J_{\text{load}} - J_{\text{sky}})}{P_{\text{load}} \left(1 + \frac{J_{\text{load}} - J_{\text{sky}}}{T_0 + J_{\text{sky}}}\right) - P_{\text{sky}}} \approx J_{\text{load}} \quad (61)$$

So

$$R \approx 1 + \frac{J_{\text{load}}(T_0 - T)}{(T + J_{\text{sky}})(T_0 + J_{\text{sky}})} \quad (62)$$

Hence, to obtain a precision y on the calibration, it is required to know the saturation temperature T_{sat} with a precision

$$\frac{\delta T_{\text{sat}}}{T_{\text{sat}}} \approx y \frac{T_{\text{sat}}}{J_{\text{load}}} \quad (63)$$

or (equivalently)

$$\frac{\delta \left(\frac{1}{T_{\text{sat}} + J_{\text{sky}}} \right)}{\left(\frac{1}{T_{\text{sat}} + J_{\text{sky}}} \right)} = y \frac{T_{\text{sat}} + J_{\text{sky}}}{J_{\text{load}}} \quad (64)$$

D Appendix: Error on the saturation temperature

Let T_0 the true saturation temperature and f_0 the true absorption of the vane. The measured saturation temperature T is given from the measured absorption f by (cf Eq.33

$$T = \frac{f(P_{\text{load}} - P_{\text{vane}})(J_{\text{load}} - J_{\text{sky}})}{P_{\text{vane}} - P_{\text{sky}} - f(P_{\text{load}} - P_{\text{sky}})} - J_{\text{sky}} \quad (65)$$

Now we use

$$P_x = \frac{T_0 J_x}{T_0 + J_x} \quad (66)$$

$$T + J_{\text{sky}} = \frac{f\left(\frac{T_0 J_{\text{load}}}{T_0 + J_{\text{load}}} - \frac{T_0 J_{\text{vane}}}{T_0 + J_{\text{vane}}}\right)(J_{\text{load}} - J_{\text{sky}})}{\frac{T_0 J_{\text{vane}}}{T_0 + J_{\text{vane}}} - \frac{T_0 J_{\text{sky}}}{T_0 + J_{\text{sky}}} - f\left(\frac{T_0 J_{\text{load}}}{T_0 + J_{\text{load}}} - \frac{T_0 J_{\text{sky}}}{T_0 + J_{\text{sky}}}\right)} = f \frac{A}{B} \quad (67)$$

Let us multiply the numerator A and denominator B by $(T_0 + J_{\text{load}})(T_0 + J_{\text{vane}})(T_0 + J_{\text{sky}})$

$$\begin{aligned} A &= [T_0 J_{\text{load}}(T_0 + J_{\text{vane}}) - T_0 J_{\text{vane}}(T_0 + J_{\text{load}})](T_0 + J_{\text{sky}})(J_{\text{load}} - J_{\text{sky}}) \\ &= T_0^2(J_{\text{load}} - J_{\text{vane}})(T_0 + J_{\text{sky}})(J_{\text{load}} - J_{\text{sky}}) \end{aligned} \quad (68)$$

$$\begin{aligned} B &= T_0 J_{\text{vane}}(T_0 + J_{\text{sky}})(T_0 + J_{\text{load}}) - T_0 J_{\text{sky}}(T_0 + J_{\text{vane}})(T_0 + J_{\text{load}}) \\ &\quad + f [T_0 J_{\text{load}}(T_0 + J_{\text{sky}})(T_0 + J_{\text{vane}}) - T_0 J_{\text{sky}}(T_0 + J_{\text{vane}})(T_0 + J_{\text{load}})] \end{aligned} \quad (69)$$

$$B = T_0^2(T_0 + J_{\text{load}})(J_{\text{vane}} - J_{\text{sky}}) - f T_0^2(T_0 + J_{\text{vane}})(J_{\text{load}} - J_{\text{sky}})$$

$$T + J_{\text{sky}} = f \frac{(J_{\text{load}} - J_{\text{vane}})(T_0 + J_{\text{sky}})(J_{\text{load}} - J_{\text{sky}})}{(T_0 + J_{\text{load}})(J_{\text{vane}} - J_{\text{sky}}) - f(T_0 + J_{\text{vane}})(J_{\text{load}} - J_{\text{sky}})} \quad (70)$$

Inserting $J_{\text{vane}} = J_{\text{sky}} + f_0(J_{\text{load}} - J_{\text{sky}})$,

$$T + J_{\text{sky}} = f \frac{(1 - f_0)(J_{\text{load}} - J_{\text{sky}})(T_0 + J_{\text{sky}})(J_{\text{load}} - J_{\text{sky}})}{(T_0 + J_{\text{load}})f_0(J_{\text{load}} - J_{\text{sky}}) - f(T_0 + J_{\text{sky}} + f_0(J_{\text{load}} - J_{\text{sky}}))(J_{\text{load}} - J_{\text{sky}})} \quad (71)$$

$$= f \frac{(1 - f_0)(J_{\text{load}} - J_{\text{sky}})(T_0 + J_{\text{sky}})}{(T_0 + J_{\text{load}})f_0 - f(T_0 + J_{\text{sky}} + f_0(J_{\text{load}} - J_{\text{sky}}))} \quad (72)$$

Let us look at the inverse of this expression

$$\frac{1}{T + J_{\text{sky}}} = \frac{(T_0 + J_{\text{load}})f_0 - f(T_0 + J_{\text{sky}} + f_0(J_{\text{load}} - J_{\text{sky}}))}{f(1 - f_0)(J_{\text{load}} - J_{\text{sky}})(T_0 + J_{\text{sky}})} \quad (73)$$

and insert $f = f_0 + \delta f$ (with $\delta f \ll f$) into it

$$\frac{1}{T + J_{\text{sky}}} = \frac{(T_0 + J_{\text{load}})f_0 - (f_0 + \delta f)(T_0 + J_{\text{sky}} + f_0(J_{\text{load}} - J_{\text{sky}}))}{f_0(1 - f_0)(J_{\text{load}} - J_{\text{sky}})(T_0 + J_{\text{sky}})} \left(1 - \frac{\delta f}{f_0}\right) \quad (74)$$

$$\begin{aligned} \frac{1}{T + J_{\text{sky}}} &= \left(1 - \frac{\delta f}{f_0}\right) \frac{(T_0 + J_{\text{load}})f_0 - f_0(T_0 + J_{\text{sky}} + f_0(J_{\text{load}} - J_{\text{sky}}))}{f_0(1 - f_0)(J_{\text{load}} - J_{\text{sky}})(T_0 + J_{\text{sky}})} \\ &\quad - \delta f \frac{(T_0 + J_{\text{sky}} + f_0(J_{\text{load}} - J_{\text{sky}}))}{f_0(1 - f_0)(J_{\text{load}} - J_{\text{sky}})(T_0 + J_{\text{sky}})} \end{aligned}$$

$$\frac{1}{T + J_{\text{sky}}} = \left(1 - \frac{\delta f}{f_0}\right) \frac{1}{T_0 + J_{\text{sky}}} - \delta f \frac{(T_0 + J_{\text{sky}} + f_0(J_{\text{load}} - J_{\text{sky}}))}{f_0(1 - f_0)(J_{\text{load}} - J_{\text{sky}})(T_0 + J_{\text{sky}})} \quad (75)$$

$$\frac{1}{T + J_{\text{sky}}} = \frac{1}{T_0 + J_{\text{sky}}} \left(1 - \delta f \left(1 + \frac{(T_0 + J_{\text{sky}} + f_0(J_{\text{load}} - J_{\text{sky}}))}{f_0(1 - f_0)(J_{\text{load}} - J_{\text{sky}})}\right)\right) \quad (76)$$

$$\frac{1}{T + J_{\text{sky}}} = \frac{1}{T_0 + J_{\text{sky}}} \left(1 - \delta f \frac{T_0 + J_{\text{sky}} - f_0^2(J_{\text{load}} - J_{\text{sky}})}{f_0(1 - f_0)(J_{\text{load}} - J_{\text{sky}})}\right)$$

Hence, to first order

$$\frac{\delta \left(\frac{1}{T_{\text{sat}} + J_{\text{sky}}} \right)}{\left(\frac{1}{T_{\text{sat}} + J_{\text{sky}}} \right)} = \frac{\delta f}{f} \frac{T_{\text{sat}} + J_{\text{sky}}}{(1-f)(J_{\text{load}} - J_{\text{sky}})} \quad (77)$$